HHS Public Access

Author manuscript

Nat Immunol. Author manuscript; available in PMC 2017 January 04.

Published in final edited form as:

Nat Immunol. 2016 August ; 17(8): 976–984. doi:10.1038/ni.3494.

Activin A programs human T_{FH} cell differentiation

Michela Locci[1], **Jennifer Wu**[1], **Fortuna Arumemi**[1], **Zbigniew Mikulski**[2], **Carol Dahlberg**[3], **Andrew T. Miller**[3], and **Shane Crotty**[1,4,5]

[1]Division of Vaccine Discovery, La Jolla Institute for Allergy and Immunology (LJI), La Jolla, CA 92037, USA

[2]Microscopy Core Facility, La Jolla Institute for Allergy and Immunology (LJI), La Jolla, CA 92037, USA

[3]Genomics Institute of the Novartis Research Foundation (GNF), La Jolla, CA 92121, USA

[4]Department of Medicine, School of Medicine, University of California, San Diego, La Jolla, CA 92037, USA

[5]Center for HIV/AIDS Vaccine Immunology and Immunogen Discovery (CHAVI-ID), La Jolla, CA 92037, USA

SUMMARY

Follicular helper T (T_{FH}) cells are $CD4^+$ T cells specialized in helping B cells and are associated both with protective antibody responses and autoimmune diseases. The promise of targeting T_{FH} cells therapeutically has been limited by fragmentary understanding of extrinsic signals regulating human T_{FH} cell differentiation. A screen of a human protein library identified activin A as new regulator of T_{FH} cell differentiation. Activin A orchestrated expression of multiple T_{FH}-associated genes, independently or in concert with additional signals. T_{FH} programming by activin A was antagonized by the cytokine IL-2. Activin A's capacity to drive T_{FH} cell differentiation *in vitro* was conserved for non-human primates but not mice. Finally, activin A-induced T_{FH} programming was dependent on SMAD2 and SMAD3 signaling and blocked by pharmacological inhibitors.

Antibody responses are a powerful arm of the adaptive immune system to prevent and fight pathogen infections. In order to produce antibodies with high affinity and pathogen neutralization potential, naïve B cells are activated and divide in response to cognate antigen and subsequently undergo rounds of somatic hypermutation and selection in germinal centers (GC), which are specialized microanatomical sites in secondary lymphoid organs.

Correspondence should be addressed to S.C. (shane@lji.org).

Accession codes

GEO: RNA-seq datasets, GSE78276.

AUTHOR CONTRIBUTIONS

M.L. and S.C. conceived and designed the experiments; M.L. and J.W. performed experiments and analyzed data; F.A. performed SMAD-related experiments; Z.M. generated and analyzed immunofluorescence data; C.D. contributed to the screen optimization; A.T.M. provided the secretomics library; M.L. and S.C. wrote the paper; S.C. supervised the study.

COMPETING FINANCIAL INTERESTS

The authors declare no competing financial interest.

This process of affinity maturation is tightly regulated by follicular helper T (T_{FH}) cells[1–3], a distinct subset of $CD4^+$ T cells specialized in helping B cells. T_{FH} cells provide signals for selection, survival and proliferation of GC B cells via cytokine production and costimulatory molecule expression[4]. T_{FH} cell help to B cells has been found to be a limiting factor for determining the magnitude of germinal center reactions and the mutation rate of GC B cells[1, 5].

The distinctive features of T_{FH} cells are acquired during a multi-stage, multi-factorial differentiation process that takes place in secondary lymphoid organs[1, 6, 7]. Upon priming of naïve $CD4^+$ T cells by DCs or other myeloid antigen presenting cells (APCs), activated antigen-specific $CD4^+$ T cells may upregulate the chemokine receptor CXCR5 and become early T_{FH} cell precursors. The activated $CXCR5^+$ $CD4^+$ T cells migrate towards the B cell follicles upon downregulation of chemokine receptor CCR7. At this early stage of differentiation, the $CXCR5^{int}CCR7^{lo}$ T_{FH} cells can be found at the border between T cell area and B cell follicles (T cell-B cell border) and in B cell follicles. Here, T_{FH} cells interact with cognate B cells, which deliver stimuli to T_{FH} cells to complete their differentiation. Fully polarized GC T_{FH} cells are located within GCs and highly express CXCR5 ($CXCR5^{hi}$) and the T_{FH} lineage defining transcription factor Bcl6[1, 6]. GC T_{FH} cells are functionally mature B cell helpers, expressing high levels of canonical functional mediators (interleukin 21 (IL-21), CXCL13, CD40L, ICOS, SLAMF1, interleukin 4 (IL-4)), along with a series of inhibitory receptors (PD-1, BTLA, and others), which restrain T_{FH} cells from excessive proliferation[1, 4].

Multiple signaling pathways cooperate to imprint the T_{FH} differentiation program. Over the past decade, roles for the costimulatory receptor ICOS, interleukin 6 (IL-6), IL-21, interleukin 2 (IL-2), SLAM family receptors, and other molecules were shown to regulate mouse T_{FH} cell differentiation[1, 6]. However, few studies identified regulators of human T_{FH} biology. Interestingly, some data suggest evolutionary divergences between the signaling pathways shaping human and mouse T_{FH} cell differentiation. IL-6 is the dominant inducer of murine IL-21 production and an important early regulator of T_{FH} differentiation in mice[8–11], but it has minimal effects on human $CD4^+$ T cell IL-21 induction and *in vitro* T_{FH} cell generation[12]. In contrast, interleukin 12 (IL-12) is a potent regulator of IL-21 production and T_{FH} cell differentiation in humans[13, 14], but it has only a minor effect on mouse $CD4^+$ T cell IL-21 expression[8, 15]. Thus, while extremely valuable for studies of evolutionarily shared pathways, mice might represent a limited model for identification of regulators of human T_{FH} cell differentiation. In light of those apparent differences, we developed an *in vitro* screen of a large human recombinant protein collection to uncover novel regulators of human T_{FH} cell differentiation.

RESULTS

Screen for novel regulators of human T_{FH} differentiation

To discover novel regulators of human T_{FH} cell differentiation, we performed an unbiased high-throughput screen of a human extracellular proteome library consisting of over 2000 human proteins predicted or known to be cytokines, chemokines, morphogens, costimulatory receptors, or single pass transmembrane molecules[16]. Each unique protein in

this proteome, or 'secretomics', library was produced as a secreted recombinant molecule and tested for its capacity to modulate the differentiation of activated naïve $CD4^+$ T cells into T_{FH} cells *in vitro* (Supplementary Fig. 1a and Supplementary Fig. 1b). Briefly, activated human naïve $CD4^+$ T cells were cultured for 5d in the presence of the human secretome library in duplicate. Expression of the T_{FH} cell signature markers CXCR5 and PD-1 were measured by flow cytometry, in an automated fashion. The primary screen revealed multiple recombinant proteins that either induced or inhibited CXCR5 and PD-1 expression, as identified by PD-1^+CXCR5^+ cell % (Fig. 1a) or CXCR5^+ cell % (Supplementary Fig. 1c) ranked by *z*-score. Eleven members of the type I interferon cytokine family, known inhibitors of mouse[17] and human[12] T_{FH} cell differentiation, were identified in the primary screen as suppressors of CXCR5 and PD-1 expression (Fig. 1a). Activin A, the inhibin beta A (INHBA) homodimer, emerged as the most potent inducer of CXCR5 and PD-1 (Fig. 1a). We then confirmed the primary screen results, showing that activin A induces CXCR5 and PD-1 expression (Fig. 1b).

Activin A belongs to the family of activins-inhibins, a group of five distinct dimeric cytokines that can arise from three monomer subunits, inhibin alpha, beta A, beta B[18]. Activin A is a pleiotropic cytokine involved in multiple vital biological processes, including maintenance of pluripotent stem cells[19–23]. However, the role of activin A in the immune system is not fully understood, with only a small number of studies providing evidence for involvement of activin A in T cell biology[22, 24–26]. We evaluated the presence of activin A in human tonsils, a lymphoid tissue enriched in T_{FH} cells and GCs where T_{FH} cell differentiation physiologically occurs. INHBA protein was found in T cell zones, including the T cell-B cell borders, of all tonsils analyzed (Fig. 2a and Supplementary Fig. 2a). INHBA$^+$ T cells were observed. The strongest INHBA production was in $CD3^-$ cells with myeloid cell morphology, consistent with the known ability of monocytes, dendritic cells (DCs) and macrophages to produce activin A[27–29]. CD11c staining revealed both CD11c$^+$ and CD11c$^-$ cells expressing INHBA in T cell areas (Fig. 2b and Supplementary Fig. 2b). Furthermore, blood monocytes upregulated *INHBA* expression within 4h following LPS stimulation, and secreted activin A protein (Fig. 2c,d), confirming that human APCs are capable of activin A production.

The role of activin A in *in vitro* T_{FH} cell differentiation was then validated using primary naïve $CD4^+$ T cells from numerous human donors (Fig. 3a–c) and activin A from multiple commercial vendors (data not shown). Furthermore, serum-free medium was used throughout these validation experiments to rule out possible indirect effects of undefined serum components. In stringent serum free conditions, activin A induced both PD-1 and CXCR5 expression on activated naïve $CD4^+$ T cells in a dose dependent fashion (Fig. 3a,b and Supplementary Fig. 3a), demonstrating a direct effect of activin A on human T_{FH} cell differentiation. Overall, these data indicate that a screen of human proteins enables the identification of factors that can function as early regulators of human T_{FH} cell differentiation, with activin A identified as the top hit in the screen.

Activin A activity is modulated by IL-12 family members

IL-12 is the strongest identified IL-21 inducer for human $CD4^+$ T cells[13, 14]. IL-12 can also modulate CXCR5 expression[30]. Therefore, we asked whether IL-12 might act in synergy with activin A. Activin A regulation of CXCR5 was enhanced by IL-12 (Fig. 3a,b). Expression of CXCR5 and PD-1 was retained by cells stimulated with activin A in combination with IL-12 for 10d of *in vitro* culture (Fig. 3c). Two additional IL-12 cytokine family members, IL-23 and IL-35, were also evaluated. IL-23 had a small activity in combination with activin A, while IL-35 had no relevant effect on CXCR5 and PD-1 expression in serum-free conditions (Supplementary Fig. 3c,d).

Treatment of activated $CD4^+$ T cells with an activin A neutralizing monoclonal antibody abolished differentiation of $PD\text{-}1^+CXCR5^+$ cells at a range of activin A concentrations (Fig. 3d and Supplementary Fig. 3b). Activin A primarily binds and signals through the type I receptor ACVR1B (ALK4), in complex with the activin A receptor type IIA (ACVR2A) or IIB (ACVR2B)[31, 32]. A monoclonal antibody against both human Type II activin A receptors ('pan anti-ACVR2') resulted in a severe decrease of PD-1 and CXCR5 induction driven by activin A (Fig. 3d). Thus, activin A acts directly on activated human $CD4^+$ T cells and regulates PD-1 and CXCR5 expression in a Type II activin A receptor-specific manner.

Instruction of a human T_{FH} gene program by activin A

Since activin A promoted expression of the canonical T_{FH} markers PD-1 and CXCR5, we asked if activin A, alone or in combination with IL-12, likewise regulated expression of additional molecules known to be important for T_{FH} cell biology. Activin A was sufficient to decrease CCR7 expression on activated $CD4^+$ T cells (Fig. 3e). Moreover, a fraction of $CD4^+$ T cells differentiated with activin A plus IL-12 increased expression of Bcl6 (Fig. 3f and Supplementary Fig. 4a,b). Next, we ascertained the global transcriptomic profile of the *in vitro* differentiated T_{FH}-like cells by RNA sequencing (RNA-seq). A comparison of gene expression profiles of *in vitro* cultured $CD4^+$ T cells and *bona fide* human GC T_{FH} cells revealed that cells differentiated in presence of activin A or activin A plus IL-12 were imprinted with *bona fide* GC T_{FH} signature genes (activin A+IL-12 versus "−": FDRq=0.015, Fig. 3g–i). Activin A contributed more than IL-12 to driving expression of GC T_{FH} associated genes (activin A+IL-12 versus IL-12: p=0.046; activin A+IL-12 versus activin A: p=0.14, Fig. 3h,i). Activin A plus IL-12 resulted in selective upregulation of 116 genes versus cells differentiated with beads only (Fig. 3j and Supplementary Table 1), including several T_{FH}-associated genes such as *SLAMF1, LIF, LTA*, and *TNF* (Fig. 3k and Supplementary Fig. 5), in addition to *CXCR5* and *PDCD1* (PD-1). Activin A emerged as the major factor regulating *LIF, LTA, PDCD1*, and *TNF* genes (Fig. 3k). Differential *LIF* and SLAMF1 expression were confirmed (Fig. 3l,m).

In addition to the upregulated genes, a set of 60 genes was suppressed by activin A plus IL-12 (Fig. 3j and Supplementary Table 2). Activin A caused significant downregulation of *PRDM1*, which encodes the transcription factor Blimp-1 (Fig. 3k,n). Blimp-1 is a potent and well-established Bcl6 antagonist that is expressed at low levels in bona fide T_{FH} cells[1]. *ITGB7*, which encodes integrin β_7 and is expressed at low levels on human GC T_{FH} cells (Supplementary Fig. 5), was downregulated in the presence of activin A (Fig. 3o).

Altogether, gene expression analysis indicated that activin A is sufficient to regulate expression of multiple molecules important for T_{FH} cell biology, including genes involved in migration, differentiation, and proliferation.

Activin A regulation of T_{FH} cell function

T_{FH} cells are defined by their specialized function as B cell helpers. To investigate whether activin A can modulate T_{FH} cell function, we evaluated production of canonical T_{FH} lymphokines by the *in vitro* differentiated cells. CXCL13, the chemokine ligand of CXCR5, exhibits cytokine-type activity on B lymphocytes[33] and is one of the defining factors secreted by human T_{FH} cells. CXCL13 is constitutively produced in large quantities by human GC T_{FH} cells and is selectively expressed by circulating memory T_{FH} cells upon restimulation[34–36]. Activin A selectively induced CXCL13 expression by $CD4^+$ T cells *in vitro* (Fig. 4a).

IL-21 is a cytokine highly produced by GC T_{FH} cells and circulating memory T_{FH} cells[36, 37]. IL-21 regulates GC B cell survival and plasma cell differentiation[4, 38]. As expected, $CD4^+$ T cells cultured *in vitro* with IL-12 produced IL-21 after a short re-stimulation with PMA plus ionomycin (Fig. 4b). Moreover, cells cultured with activin A plus IL-12 retained full IL-21 production potential (Fig. 4b). Activin A cultured $CD4^+$ T cells expressed elevated amounts of TNF and LTα proteins upon restimulation (Fig. 4c,d), consistent with the RNA-seq data. Finally, we evaluated the capacity of activin A differentiated cells to provide help to B cells. $CD4^+$ T cells differentiated with activin A plus IL-12 were functionally competent B cell helpers, capable of supporting B cell proliferation and survival, plasmablast differentiation, and IgG production (Fig. 4e).

Overall, our data indicate that activin A, in combination with IL-12, promotes the generation of T_{FH}-like cells that express high levels of CXCR5 and PD-1, modulate expression of Bcl6, *PRDM1*, CCR7, ITGB7, and SLAMF1, and display T_{FH} functional properties, including B cell helper activity and production of CXCL13, IL-21, TNF, and LTα

Activin A-TGF-βrelationship in T_{FH} differentiation

Transforming growth factor beta (TGF-β is a pleiotropic cytokine involved in the differentiation of multiple $CD4^+$ T cell subsets in a context dependent fashion[39]. A recent study showed that TGF-β in conjunction with IL-12 and other cytokines, played a role in human T_{FH} cell differentiation[12]. While activin A and TGF-β use independent receptors, both cytokines can trigger SMAD2/3 signaling pathways downstream of their respective receptors[31, 32, 39]. We utilized stringent serum-free conditions and found that TGF-β synergized with IL-12 to induce CXCR5 and PD-1 protein expression in activated naïve $CD4^+$ T cells cultured *in vitro* for 5d (Supplementary Fig. 6a). While a T_{FH} gene signature was present in RNA-seq of the serum-free cultures, a T_H17 gene signature[12] was not observed (data not shown). TGF-β and activin A displayed a similar capacity to regulate the differentiation of PD-$1^+$$CXCR5^+$ and $Bcl6^+$ cells (Supplementary Fig. 6b) when combined with IL-12. A comparison of activin A plus IL-12 versus TGF-β plus IL-12 revealed a high degree of similarity (Fig. 5a,b). “Volcano” plot analysis indicated that the majority of the genes selectively regulated by activin A plus IL-12 in comparison to beads only controls

followed the same trend as the genes regulated by TGF-β plus IL-12 versus beads only controls(Fig. 5b).

Activated $CD4^+$ T cells are capable of secreting activin A following TCR stimulation[26]. Because TGF-β mirrored activin A in driving human T_{FH} cell differentiation, we explored the possibility that activin A accounted for the TGF-β-induced phenotype *in vitro*. However, activin A blockade did not alter the frequency of PD-1^+CXCR5^+ cells induced by TGF-β (Fig. 5c), indicating that activin A is not responsible for TGF-β induced T_{FH} cell differentiation. Conversely, anti-TGF-β did not have any relevant effect on activin A–mediated T_{FH} cell differentiation, suggesting that TGF-β is not responsible for activin A-induced T_{FH} cell differentiation (Fig. 5d,e). Next, we evaluated if these two cytokines could induce PD-1 and CXCR5 expression in an additive or synergistic fashion. Neither PD-1 nor CXCR5 expression changed when activin A and TGF-β were combined *in vitro* (Fig. 5f,g). Despite driving highly similar gene expression, activin A and TGF-β significantly differed in their ability to induce Foxp3 expression, with activin A being less potent than TGF-β in driving the generation of $Foxp3^+$ cells (Fig. 5h,i). Differential induction of Foxp3 may be important *in vivo*, since Foxp3 is the lineage defining transcription factor of regulatory T (T_{reg}) cells. Thus, TGF-β may preferentially bias cells toward a T_{reg} phenotype and activin A may bias cells toward a T_{FH} phenotype. In summary, activin A and TGF-β do not account for each other's ability to regulate T_{FH} biology, and TGF-β preferentially induces Foxp3.

IL-2 modulation of activin A-mediated T_{FH} cell differentiation

We noted that *PRDM1* was expressed by activated human $CD4^+$ T cells, and that *PRDM1* expression was lower in activin A-stimulated T cells. Blimp-1 is one of the strongest negative regulators of T_{FH} differentiation, through its abilities to antagonize Bcl6 and directly suppress *CXCR5* expression[1, 40]. IL-2 potently induces Blimp-1 in mouse $CD4^+$ T cells[40–42]. We considered that reduced Blimp-1 expression may be occurring via suppression of CD25 expression, but RNA-seq data revealed no difference in *IL2RA* in the presence of activin A (data not shown). We hypothesized that $CD4^+$ T cell secreted IL-2 may be inhibiting activin A induction of T_{FH} differentiation. Therefore, we evaluated the effect of IL-2 blockade on activin A treated $CD4^+$ T cells. In the presence of activin A alone, differentiation of PD-1^+CXCR5^+ cells was remarkably increased when IL-2 was neutralized (Fig. 6a–c). IL-2 blockade also modestly potentiated the expression of PD-1 and CXCR5 in cells cultured with activin A plus IL-12 (Supplementary Fig. 7). Thus, IL-2 is a potent inhibitor of human T_{FH} cell differentiation, and activin A can directly induce human T_{FH}-associated gene expression in the absence of any additional cytokines.

Evolutionary requirement for activin A in T_{FH} differentiation

To test the functional conservation of activin A in T_{FH} differentiation, we activated murine naïve $CD4^+$ T cells in the presence of activin A alone or combined with IL-12. The activin A amino acid sequence is 100% conserved between human and mouse. Strikingly, activin A did not have any effect on PD-1 and CXCR5 expression by mouse $CD4^+$ T cells (Fig. 7a,b). This was true for both C57BL/6 and BALB/c mouse strains (Fig. 7a,b). The presence of IL-6, a known regulator of early murine *in vivo* T_{FH} cell differentiation, in combination with activin A did not promote *in vitro* mouse T_{FH} cell differentiation (Fig. 7b).

The lack of any measurable effect of activin A on T_{FH}-associated gene expression by mouse $CD4^+$ T cells prompted us to investigate whether the role of activin A in T_{FH} differentiation was unique to humans. Thus, we evaluated the capacity of activin A to drive *in vitro* T_{FH} cell differentiation by a species in a different taxonomical family, *macaca mulatta* (rhesus macaques) of the non-human primate family Cercopithecidae. Potent induction of $PD\text{-}1^+CXCR5^+$ cells was observed by activated *m. mulatta* naïve $CD4^+$ T cells in response to activin A (Fig. 7c,d). These data indicate that the T_{FH}-like differentiation mediated by activin A *in vitro* is not preserved in mice, but is conserved between non-primate species and humans. This finding suggests the existence of a possible evolutionary divergence in activin A-mediated T_{FH} cell differentiation.

SMAD2/3 pathway in activin A-induced T_{FH} differentiation

SMAD2/3 is the canonical signaling pathway activated downstream of activin A binding to type IIA and/or IIB receptors and type I receptor ACVR1B (ALK4)[31, 32]. Phosphorylation of SMAD2/3 occurred in naïve human $CD4^+$ T cells in response to activin A (Fig. 8a,b). Potential SMAD-independent pathways downstream of activin A were not observed (Supplementary Fig. 8). Therefore, we hypothesized that SMAD2/3 activation is a central signaling pathway in activin A mediated induction of T_{FH}-associated gene expression. A pharmacological inhibitor of ALK4, SB431542, known to suppress SMAD2/3 activation but not the SMAD-independent pathways[43], resulted in complete inhibition of activin A-mediated SMAD2/3 phosphorylation (Fig. 8a,b). Furthermore, ALK4 inhibition by SB431542 blocked the differentiation of $PD\text{-}1^+CXCR5^+$ cells in activin A containing culture conditions (Fig. 8c,d). Galunisertib[44] is an independent small molecule ALK4 inhibitor currently in clinical trials. Galunisertib potently suppressed $PD\text{-}1^+CXCR5^+$ cell generation in response to activin A (Fig. 8e and Supplementary Fig. 8c). Altogether, these data point to SMAD2/3 as an important signaling pathway downstream of activin A in the regulation of human T_{FH} cell differentiation.

Activin A is expressed in human lymphoid tissue in both the T cell area and the T cell-B cell border area. We observed a gradient in activin A induction of phosphorylated SMAD2/3 in tonsillar $CD4^+$ T cells, with naïve $CD4^+$ T cells having the highest responsiveness to activin A (Fig. 8f,g). $PD\text{-}1^{int}CXCR5^{int}$ $CD4^+$ T cells, a heterogeneous population of T_{FH}-associated cells located at the T cell-B cell border and in the follicular mantle (mantle T_{FH}, mT_{FH}), also induced SMAD phosphorylation in response to activin A (Fig. 8f,g), although to a lesser extent than naïve $CD4^+$ T cells. This reduced responsiveness might at least partially be explained by a trend of lower expression of the activin A Type I and II receptors in differentiated T_{FH} cells in comparison to naïve $CD4^+$ T cells (Supplementary Fig. 8d). The tonsillar expression pattern of activin A receptors is consistent with the finding that naïve $CD4^+$ T cells from blood expressed *ACVR1B, ACVR2A* and *ACVR2B*, but that following TCR stimulation the activin A receptors were down regulated (Fig. 8h). The presence of activin A did not influence the reduction in Type I and II activin A receptors driven by TCR triggering (Fig. 8i). In summary, activin A is expressed by myeloid cells in areas where T_{FH} cell differentiation is initiated, and $CD4^+$ T cells in those locations are responsive to activin A signaling, consistent with an in vivo role for activin A as an early regulator of human T_{FH} cell differentiation.

DISCUSSION

This work establishes a role for activin A in human T_{FH} differentiation. Proper localization is a key feature of T_{FH} biology. Activin A acts by dampening CCR7 and ITGβ7 while fostering CXCR5 expression. Besides regulating localization, activin A also modulates the expression of T_{FH} functional regulators. Activin A promotes the production of CXCL13, TNF, LIF, and LTα. TNF can act as co-stimulatory signal to mediate B cell activation and Ig production[38]. The roles of LIF and LTα in B cell help have not been formally addressed. However, B cell hyperplasia and polyclonal hypergammaglobulemia are found in mice overexpressing LIF[45]. In T cell-B cell co-cultures, the B cell helper activity of the *in vitro* differentiated T_{FH} cells was driven by IL-12. This assay has major limitations in that it mostly relies on CD40L (comparably expressed by all activated $CD4^+$ T cells *in vitro*) and IL-21. Therefore, T_{FH} cell features regulated by activin A vital for B cell helper function *in vivo*, such as CXCL13 and cell migration (CXCR5, CCR7) are not emphasized in the available assay.

One important open question is whether activin A and TGF-β physiological distribution indicates which of these two cytokines is more relevant for Tfh differentiation *in vivo*. There are many means by which TGF-β *in vivo* bioavailability is regulated, including the fact that TGF-β is physiologically activated in an extremely localized fashion by integrin expressing cells[39]. Activin A bioavailability is regulated differently[31, 32]. Therefore, it is not currently possible to predict if activin A or TGF-β is more dominant at inducing Tfh differentiation in a particular *in vivo* context. Clearly activin A is present in human lymphoid tissue and is induced in myeloid cells by inflammatory TLR ligands. It is still controversial as to whether acquisition of Foxp3 *in vitro* by human $CD4^+$ T cells confers them with the capacity to suppress immune responses[46]. Nevertheless, lower Foxp3 induction by activin A in comparison to TGF-β appears to be a favorable event when the ultimate goal is the induction induce human Tfh cells.

Activin A alone was sufficient for the regulation of many Tfh signature molecules, particularly in the absence of high IL-2. Nevertheless, integration of activin A and IL-12 mediated signals was required to acquire a more complete phenotype, including high IL-21 expression. These findings support a working model in which activin A is at the center of a cytokine network orchestrating human Tfh cell differentiation. The cytokine network includes not only additional agonistic players such as IL-12, but also antagonistic signals such as IL-2. We envision the cytokine network driving Tfh cell differentiation to be more complex than what has been described so far.

A significant limitation in the usage of rodent models results from the existence of evolutionary divergence in pathways shaping T_{FH} biology. Fully mature mouse and human T_{FH} cells express a virtually identical set of signature molecules. Despite the phenotypical similarity, a growing body of evidence suggested that there are signaling pathways crucial for human, but not mouse, T_{FH} cell differentiation. Three recent studies reported different outcomes on mouse T_{FH} cell differentiation when TGF-β signaling was impaired, with one study finding that TGF-β is a positive regulator of T_{FH} biology by virtue of its ability to insulate $CD4^+$ T cells from IL-2 signaling and suppress Th1 differentiation[47]. A second

study, however, found no effect on T_{FH} cells when TGF-β signaling was blocked[48]. Finally, a third study indicated that TGF-β behaved as a T_{FH} cell inhibitor[49]. Additional studies are therefore required to clarify TGF-β's role in T_{FH} biology in mice. While we could not find any relevant effect of activin A on mouse $CD4^+$ T cells *in vitro*, activin A potently induced human and non-human primate T_{FH} differentiation. These data suggest the existence of a potential evolutionary divergence in the role that activin A plays in T_{FH} cell biology. Alternatively, the inability of activin A to induce mouse $CD4^+$ T cell T_{FH} differentiation *in vitro* may reflect an unknown inhibitor or cofactor.

It is highly desirable to foster T_{FH} cells *in vivo* for vaccines, when the generation of a protective vaccine relies on the production of neutralizing antibodies[1]. Memory T_{FH} cells and recently activated T_{FH}-related cells can be found in blood[1, 7, 35–37, 50]. Highly functional memory T_{FH} cells were the strongest immunological correlate for HIV broadly neutralizing antibody development among HIV^+ donors[36]. In contrast, dysregulated antibody responses may lead to auto-antibody mediated diseases[3, 7] and memory T_{FH} cells are perturbed in rheumatoid arthritis, systemic lupus erythematous and juvenile dermatomyositis[3, 7, 37]. In these contexts, hampering T_{FH} cells in a targeted fashion represents a promising therapeutic approach. An appealing candidate could be Galunisertib[44], which is currently being tested in clinical trials.

In conclusion, our study revealed a powerful approach for identification of novel regulators of human T_{FH} cell differentiation, which led to the discovery of activin A as potent regulator of human T_{FH} cell differentiation.

METHODS

Human samples

Leukapheresis sample from a healthy donor was obtained from AllCells, Inc., after a prescreening of multiple donors. Fresh whole blood samples from healthy donors were obtained from the La Jolla Institute for Allergy and Immunology (LJI) in-house normal blood donor program (NBDP). Informed consent was obtained from all donors. Fresh human tonsils were obtained from the National Disease Resource Interchange. Tonsil preparation was previously described[34]. All the protocols were approved by LJI institutional review board. Peripheral blood mononuclear cells (PBMCs) were isolated from both leukapheresis and whole blood samples by density-gradient centrifugation using Histopaque-1077 (Sigma-Aldrich).

Mouse samples

C57BL/6J and BALB/cJ mice were from Jackson Laboratory. Mice were housed in specific pathogen–free conditions in accordance with the Institutional Animal Care and Use Guidelines of the La Jolla Institute.

Non-human primate samples

All rhesus macaque study procedures were performed in accordance with Emory School of Medicine Institutional Animal Care and Use Committee approved protocols. Previously cryopreserved macaque PBMCs were used.

Flow cytometry and cell sorting

For surface staining, primary-staining panels used for phenotypic analysis or for cell sorting are described in supplemental antibody table (Supplementary Table 3). For the intranuclear staining: cells were treated with the Foxp3 Fixation/Permeabilization kit (eBioscience) and stained in Permeabilization buffer (eBioscience). For cytokine staining: day 3 or day 5 *in vitro*-differentiated cells (specified in the main text or in figure legends) cells were stimulated for 5 h at 37°C with Phorbol 12-myristate 13-acetate (PMA, 2 5ng/ml) and Ionomycin (1 μg/ml) in the presence of Brefeldin A (5 μg/ml). Cells were fixed with PBS 2% FBS, 1% PFA and permeabilized with PBS 2% FBS, 0.5% Saponin (from quillaja bark, Sigma-Aldrich). Samples were analyzed on a LSR Fortessa Cell Analyzer (BD, Bioscience). Flow cytometry data were analyzed with FlowJo (Tree Star). For cell sorting, cells were sorted using sorted using a FACS Aria (BD, Bioscience).

Screening of 'secretomics' recombinant proteins

Naïve $CD4^+$ T cells were isolated from leukapheresis-derived mononuclear cells via CliniMACS negative selection (Miltenyi Biotec). The 'secretomics' collection was previously described[16]. An expanded secretomics set (PhaseII), composed of 2688 unique proteins (total 1772 genes) was tested. Naïve $CD4^+$ T cells (1.25×10^4 cells/well) were cultured with secretomics proteins in the presence of Dynabeads Human T-Activator CD3/CD28 (0.5 μl/well, Life Technologies), recombinant human IL-7 (4 ng/ml, Peprotech), and anti-human-TGF-β blocking antibody (100 μg/ml, clone 1D11.16.8, BioXcell) in RPMI medium (Cellgro), supplemented with 10% fetal bovine serum (Omega Scientific), GlutaMAX (Gibco) and Penicillin/Streptomycin (Gibco). Induction of CXCR5 and PD-1 was assessed after 5 d of *in vitro* culture using automated FACS acquisition via HTS on LSR Fortessa (BD Biosciences). Flow cytometry panel is listed in Supplementary Table 3. For each 384-well plate, mean and standard deviation of $PD\text{-}1^+CXCR5^+$ or $CXCR5^+$ cell frequency induced by each individual recombinant proteins was determined and used to calculate the *z*-score (value indicating how many standard deviations an element is from the mean). *Z*-scores of replicate plates were analyzed independently.

In vitro $CD4^+$ T cell differentiation

Unless differently specified, naïve $CD4^+$ T cells were enriched from PBMCs by magnetic bead negative selection with the EasySep™ Naïve $CD4^+$ T Cell Isolation Kit (STEMCELL Technologies). Purity ($CD4^+CD45RA^+$) was 90% or higher. Cells (7.5×10^4 cells/well) were activated by Dynabeads Human T-Activator CD3/CD28 (2 μl/well, Life Technologies) and cultured with recombinant human/mouse/rat activin A (50 ng/ml or 100 ng/ml), recombinant human IL-12 (5 ng/ml), recombinant human TGF-β (1 ng/ml), recombinant human IL-23 (10 ng/ml) or recombinant human IL-35 (10 ng/ml) in the presence of recombinant human IL-7 (4 ng/ml) in AIM-V medium (Life Technologies). All cytokines

were from R&D System and Peprotech. The 14 kDa mature human beta A chain of human activin A shares 100% amino acid sequence identity with bovine, feline, mouse, porcine, and rat beta A. Phenotype was quantified after 3 or 5 d, as specified in the Figure legends. Similar results were obtained when using T_{reg} cell-depleted purified naïve $CD4^+$ T cells (Supplementary Fig. 2a), in which cells were sorted from total PBMCs by flow cytometry as $CD19^-CD8^-CD14^-CD16^-CD4^+CD45RO^-CD25^-$ cells. For experiments quantifying supernatant CXCL13 concentration, cells were activated by plate-bound anti-human CD3 (5 μg/ml, BD) and ICOS-L (5 μg/ml, recombinant human B7-H2, R&D). CXCL13 concentrations were determined via human CXCL13 DuoSet ELISA (R&D) on supernatants harvested after 5 d of *in vitro* culture. For blocking experiments, cells were cultured with anti-activin A (5 μg/ml, clone 69403, R&D), pan anti-activin A Type II receptor (ACVR2) (100μg/ml, Novartis), anti-TGF-β (100μg/ml, clone 1D11.16.8, BioXcell), or equivalent concentration of mouse IgG1 isotype antibody (BioXcell). For blockade of IL-2, cells were cultured with anti-IL-2 (10μg/ml, clone 5334, R&D) or mouse IgG1 isotype antibody (BioXcell). For SMAD2/3 inhibition experiments, cells were cultured with different concentrations of SB 431542 (Tocris Bioscience), Galunisertib (LY2157299, Selleck Chemicals) or vehicle (DMSO) for 5 d in AIM-V supplemented with 2% heat-inactivated FBS or in RPMI-1640 (Corning) supplemented with 10% heat-inactivated FBS, 1% GlutaMax, 1% PenStrep.

Microscopy

Tonsils were fixed for 4 h in freshly diluted 4% paraformaldehyde in PBS (Electron Microscopy Sciences, EMS Diasum), then washed 3 times in PBS and equilibrated in 30% w/v sucrose solution in PBS for 24 h. Tissues were briefly washed in PBS, frozen in OCT and stored at −80 °C. Cryostat sections were cut at 12 μm thickness, and air-dried for 30 min. Sections were rehydrated for 10 min in PBS and non-specific binding sites were saturated with 5% normal donkey serum (Jackson Immunoresearch) in the presence of 0.3% Triton X-100 in PBS for 1 h. Tissues were incubated with rabbit polyclonal anti-INHBA (HPA020031, Sigma-Aldrich), mouse anti-CD3−FITC (UCHT1, Tonbo Biosciences) and mouse anti-Bcl6–Alexa Fluor 647 (K112-91, BD Biosciences) overnight at 4 °C. Following washing, sections were reacted with donkey anti-rabbit–Alexa Fluor 568 and goat anti-FITC–Alexa Fluor 488 secondary antibodies (Invitrogen) for 1 h at 23 °C. For CD11c staining, slides were first incubated with anti-INHBA and mouse anti-CD11c (3.9, BD), washed and reacted with donkey anti-rabbit–Alexa Fluor 568 and goat anti-mouse–DyLight 649 secondary antibodies (Biolegend). Following brief fixation slides were stained with anti-CD3 as described above. Slides were counterstained with 10 μg/ml Hoechst for 10 min, washed and mounted in Prolong Gold antifade reagent (Invitrogen) with a cover slip and examined with AxioScan Z1 slide scanner equipped in 20x/0.8 NA air objective using appropriate filter sets. High resolution imaging of selected regions was done on a FluoView FV10i confocal microscope (Olympus) using 60x/1.35 NA oil objective. To reduce blurriness epifluorescence images were processed with an extended depth of field algorithm (ZEN2, Zeiss). To improve feature visibility images were processed by contrast stretching using identical procedures (ZEN2 and Olympus FluoView software).

A separate anti-INHBA from Abcam (ab56057) was used for staining validation and comparable results were obtained. In addition, two independent rabbit IgG (R&D and EMD Millipore) and mouse IgG1 (Biolegend) were used as negative controls. Equipment and settings used to acquire microscopy data are described in Supplementary Table 4.

Monocyte stimulation

Monocytes were isolated by human peripheral blood mononuclear cells by EasySep™ human CD14-positive selection kit (STEMCELL Technologies). Purity, measured as percentage of $CD14^+$ cells by flow cytometry, was 90% or higher. For qPCR analysis of *INHBA* expression, 10^6 $CD14^+$ cells were cultured in 96-well plates, with or without *Escherichia coli*-derived LPS (100 ng/ml, Invivogen) for 4 h at 37°C and then frozen in RLT buffer (Qiagen). For quantitation of activin A secretion by ELISA, 10^6 $CD14^+$ cells were cultured in 48-well plates, with or without *E. coli*-derived LPS (100 ng/ml, Invivogen) for 48 h at 37°C. After 48 h, supernatant was collected and then frozen for subsequent measure of secreted activin A. Supernatants were diluted 1:20 and activin A was measured by Human/Mouse/Rat activin A Quantikine ELISA kit (R&D) following manufacturer instructions.

T–B co-culture

Naïve $CD4^+$ T cells were differentiated with activin A and/or IL-12. At day 3, live $CD4^+$ T cells were sorted by flow cytometry. Fresh autologous B cells were enriched from PBMCs by CD19 magnetic-bead positive selection (Miltenyi Biotec). Memory B cells were then sorted by flow cytometry as $CD3^-CD14^-CD4^-CD19^+IgD^-CD27^+$ cells as previously described[36] and cultured (4×10^5 cells/well) with the *in vitro* differentiated T cells (2.5×10^3 cells/well) in the presence of staphylococcal enterotoxin B (SEB, 0.25 ng/ml, Toxin Technology) in AIM-V medium. B cell counts and plasmablast frequencies were measured after 7 d by flow cytometry as previously described[36]. Ig concentrations in the supernatants were determined by ELISA.

Mouse $CD4^+$ T cell differentiation

Naïve $CD4^+$ T cells were isolated from spleen using the Naïve $CD4^+$ T cell isolation kit (Stem Cell). Purity was 92% or higher. Naïve $CD4^+$ T cells (2×10^5 cells/well) were cultured for 3 d with recombinant human/mouse/rat activin A (50 ng/ml, R&D Systems), recombinant mouse IL-12 (10 ng/ml, Peprotech), and/or recombinant mouse IL-6 (20 ng/ml, Peprotech) in the presence of plate-bound anti-mouse-CD3 mAb (8 μg/ml, clone 145-2C11, BioXcell) and anti-mouse-CD28 (8 μg/ml, clone 37.51, BioXcell), in RPMI medium, supplemented with 10% fetal bovine serum, GlutaMAX, penicillin/streptomycin, and 2.5 μM β-mercaptoethanol. After 3 d, cells were removed from stimuli and further cultured for 2 additional d in IL-2 (50 U/ml,) and the same cytokine combination used at day 0. Phenotype was quantified by flow cytometry (Supplementary Table 3) at day 5 of the *in vitro* culture.

Non-human primate (NHP) $CD4^+$ T differentiation

$CD4^+$ T cells from rhesus macaque PBMCs were enriched using the Non-Human Primate $CD4^+$ T Cell Isolation Kit (Miltenyi Biotec). Naïve $CD4^+$ T cells were isolated by flow cytometry as $CD4^+CD45RA^+CD95^-CD28^+CCR7^+$ cells. Naïve $CD4^+$ T cells (7.5×10^4

cells/well) were activated by plate-bound anti-human-CD3 and anti-human-CD28 (both at 5 μg/ml, BD) and cultured with recombinant human/mouse/rat activin A (50 ng/ml) and/or recombinant human IL-12 (5 ng/ml) for 5 d. Phenotype was assessed by flow cytometry, following the staining panel in Supplementary Table 3.

RNA sequencing

Differentiation of naïve $CD4^+$ T cells with activin A and/or IL-12 was described above. Naïve $CD4^+$ T cells from 4 or more donors were cultured with the following conditions: beads only (−), IL-12, activin A (100 ng/ml), activin A (100 ng/ml) + IL-12, TGF-β, TGF-β + IL-12. After 3 d of *in vitro* culture, live $CD4^+$ T cells were sorted by flow cytometry. Total RNA was purified using miRNAeasy Mini kit (Qiagen). Standard quality control steps were included to determine total RNA quality using Agilent Bioanalyzer (RNA integrity number (RIN) > 8.5; Agilent RNA 6000 Nano Kit) and quantity using a nanoliter spectrophotometer (Nanodrop, Thermofisher). For every sample, 500 ng of purified total RNA was prepared into mRNA libraries, according to manufacturer's instructions, using the Truseq Stranded mRNA Library Prep Kit (Illumina, RS-122-2103). The resulting libraries were deep sequenced, using the Illumina HiSeq2500 system in rapid run mode, to obtain between 6–7 $\times 10^6$ of 50-bp length single-end reads per library (Supplementary Table 5).

Analysis of RNA-seq data

The single-end reads that passed Illumina filters were filtered for reads aligning to tRNA, rRNA, adapter sequences, and spike-in controls. The reads were then aligned to UCSC hg19 reference genome using TopHat (v 1.4.1). DUST scores were calculated with PRINSEQ Lite (v 0.20.3) and low-complexity reads (DUST > 4) were removed from the BAM files. The alignment results were parsed via the SAMtools to generate SAM files. Read counts to each genomic feature were obtained with the htseq-count program (v 0.6.0) using the "union" option. After removing absent features (zero counts in all samples), the raw counts were converted to RPKM value followed by quantile normalization via R library 'aroma.light'. Then the quantile normalized RPKM values were filtered by setting a cutoff value of 1 and analyzed with the Multiplot module in GenePattern suite (http://www.broadinstitute.org/cancer/software/genepattern/) to generate the Volcano, Heatmap and Expression plots. Meanwhile the filtered raw counts were imported to R/Bioconductor package DESeq2 (v 3.1) to normalize counts and identify differentially expressed genes among conditions.

Gene Set Enrichment analysis (GSEA)

Gene Set Enrichment Analysis (v 2.2.0; http://www.broadinstitute.org/gsea/index.jsp) was used to evaluate if a pre-defined tonsil GC-T_{FH} gene set showed statistically significant enrichment between two phenotypes when cells are given a particular stimulus. The tonsil GC T_{FH} gene set (Supplementary Table 6) was generated from previously published microarray data[36] and defined by genes with more than two-fold higher expression in GC-T_{FH} cells ($CD4^+CD45RO^+PD\text{-}1^{hi}CXCR5^{hi}$) compared to non-$T_{FH}$ cells ($CD4^+CD45RO^+PD\text{-}1^-CXCR5^-$). For RNA-seq profiles used as the query list, genes were ranked from the most up-regulated to the most down-regulated in cells stimulated with beads versus activin A + IL-12, IL-12 versus activin A + IL-12, and activin A versus activin A + IL-12 on the basis of the DESeq2 analysis results. The signal-to-noise metric was used for

ranking the genes in the RNA-seq expression datasets and 10^5 cycles of permutations on the phenotype labels were performed to determine the normalized enrichment score (NES).

Quantitative Real-Time PCR

RNA was isolated by QIAGEN RNeasy spin columns and reverse-transcribed into cDNA using Superscript II Reverse Transcriptase (Invitrogen). Quantitative real-time PCR of *ACTB, LIF*, and *PRDM1* was performed using the following primers: *ACTB* forward, 5′-ACCTTCTACAATGAGCTGCG-3′, *ACTB* reverse, 5′-CCTGGATAGCAACGTACATGG-3′; *LIF* forward, 5′-ATACGCCACCCATGTCAC-3′, *LIF* reverse, 5′- CCACATAGCTTGTCCAGGTTG-3′; and *PRDM1* forward, 5′-TGTGGTATTGTCGGGACTTTG-3′, *PRDM1* reverse 5′-CTTTGGGACATTCTTTGGGCCTG-3′. The following primers were used to quantify the expression of *ACVR1B (ALK4), ACVR2A, ACVR2B* and *INHBA: GAPDH* forward, 5′-ACATCGCTCAGACACCATG-3′, GAPDH reverse 5′-TGTAGTTGAGGTCAATGAAGGG-3′, *ACVR1B* forward, 5′-GGAAGCAGAGATATACCAGACG-3′, *ACVR1B* reverse, 5′-AGATAATCAAACAGGGACCCG-3′, *ACVR2A* forward, 5′-CCTGGAATGAAGCATGAGAAC-3′, *ACVR2A* reverse, 5′-TTCCAAGAGACCACATTAGCC-3′, *ACVR2B* forward, 5′-GAGATCTTCAGCACACCTGG-3′, *ACVR2B* reverse, 5′-GATGTTCCCCTTGAGGTAATCC-3′, *INHBA* forward, 5′-ACGGGTATGTGGAGATAGAGG-3′, and *INHBA* reverse, 5′-TGGAAATCTCGAAGTGCAGC-3′. Real-time PCR was set up with Applied Biosystem SYBR Green Master Mix.

Analysis of phosphorylated SMAD2/3

Fresh PBMCs and tonsil mononuclear cells were serum-starved overnight in AIM-V medium. The following day, the cells ($10^{\wedge 6}$ cells/condition) were stimulated for 10, 30, 60, 120 or 180 min with activin A (400ng/ml) + vehicle (DMSO), activin A + SB 431542 (10μM, Tocris Bioscience), Galunisertib (LY2157299, 10 μg/ml, Selleck Chemicals) or vehicle only in AIM-V medium. Following stimulation, the cells were fixed in BD Phosflow™ Fix Buffer I (BD Biosciences), then permeabilized using BD Phosflow™ Perm Buffer III (BD Biosciences) following manufacture's instruction. The staining panel is provided in Supplementary Table 3.

Statistical Analysis

All the statistical analyses, unless differently specified, were done with two-tailed Wilcoxon matched-pairs signed ranked test, which does not assume Gaussian distribution of the data, but it allows the direct comparison of populations within donors. Independent experiments were repeated several times with controls. Prism 6.0 (GraphPad) was used for all analysis.

Supplementary Material

Refer to Web version on PubMed Central for supplementary material.

Acknowledgments

This work was supported by NIH grant UM1-AI100663 (S.C.), internal La Jolla Institute funding (S.C.) and internal GNF funding (A.M.). We thank the Protein Sciences Group at GNF for protein production. The content of GNF secretomics collection is proprietary. Access to the collection may be considered for further research collaboration agreements on a case-by-case basis. The NHP PBMCs samples were kindly provided by G. Silvestri (Emory University). We thank the sequencing core at La Jolla Institute for RNA-seq data generation. We acknowledge the National Disease Resource Interchange for providing tonsil samples.

REFERENCES

1. Crotty S. T Follicular Helper Cell Differentiation, Function, and Roles in Disease. Immunity. 2014; 41:529–542. [PubMed: 25367570]
2. Victora GD, Nussenzweig MC. Germinal centers. Annu Rev Immunol. 2012; 30:429–457. [PubMed: 22224772]
3. Craft JE. Follicular helper T cells in immunity and systemic autoimmunity. Nat Rev Rheumatol. 2012:1–11. [PubMed: 23229451]
4. Crotty S. A brief history of T cell help to B cells. Nat. Rev. Immunol. 2015; 15:185–189. [PubMed: 25677493]
5. Gitlin AD, Shulman Z, Nussenzweig MC. Clonal selection in the germinal centre by regulated proliferation and hypermutation. Nature. 2014; 509:637–640. [PubMed: 24805232]
6. Vinuesa CG, Cyster JG. How T cells earn the follicular rite of passage. Immunity. 2011; 35:671–680. [PubMed: 22118524]
7. Ueno H, Banchereau J, Vinuesa CG. Pathophysiology of T follicular helper cells in humans and mice. Nat Immunol. 2015; 16:142–152. [PubMed: 25594465]
8. Suto A, et al. Development and characterization of IL-21-producing CD4+ T cells. J Exp Med. 2008; 205:1369–1379. [PubMed: 18474630]
9. Nurieva RI, et al. Generation of T follicular helper cells is mediated by interleukin-21 but independent of T helper 1, 2, or 17 cell lineages. Immunity. 2008; 29:138–149. [PubMed: 18599325]
10. Eto D, et al. IL-21 and IL-6 are critical for different aspects of B cell immunity and redundantly induce optimal follicular helper CD4 T cell (Tfh) differentiation. PLoS ONE. 2011; 6:e17739. [PubMed: 21423809]
11. Choi YS, Eto D, Yang JA, Lao C, Crotty S. Cutting edge: STAT1 is required for IL-6-mediated Bcl6 induction for early follicular helper cell differentiation. J Immunol. 2013; 190:3049–3053. [PubMed: 23447690]
12. Schmitt N, et al. The cytokine TGF-β co-opts signaling via STAT3-STAT4 to promote the differentiation of human TFH cells. Nat Immunol. 2014
13. Ma CS, et al. Early commitment of naïve human CD4(+) T cells to the T follicular helper (T(FH)) cell lineage is induced by IL-12. Immunol Cell Biol. 2009; 87:590–600. [PubMed: 19721453]
14. Schmitt N, et al. Human dendritic cells induce the differentiation of interleukin-21-producing T follicular helper-like cells through interleukin-12. Immunity. 2009; 31:158–169. [PubMed: 19592276]
15. Nakayamada S, et al. Early Th1 cell differentiation is marked by a Tfh cell-like transition. Immunity. 2011; 35:919–931. [PubMed: 22195747]
16. Gonzalez R, et al. Screening the mammalian extracellular proteome for regulators of embryonic human stem cell pluripotency. Proc Natl Acad Sci USA. 2010; 107:3552–3557. [PubMed: 20133595]
17. Ray JP, et al. Transcription factor STAT3 and type I interferons are corepressive insulators for differentiation of follicular helper and T helper 1 cells. Immunity. 2014; 40:367–377. [PubMed: 24631156]
18. Gold E, Risbridger G. Activins and activin antagonists in the prostate and prostate cancer. Mol. Cell. Endocrinol. 2012; 359:107–112. [PubMed: 21787836]

19. Muttukrishna S, Tannetta D, Groome N, Sargent I. Activin and follistatin in female reproduction. Mol. Cell. Endocrinol. 2004; 225:45–56. [PubMed: 15451567]
20. Munz B, et al. The roles of activins in repair processes of the skin and the brain. Mol. Cell. Endocrinol. 2001; 180:169–177. [PubMed: 11451588]
21. Phillips DJ, de Kretser DM, Hedger MP. Activin and related proteins in inflammation: not just interested bystanders. Cytokine Growth Factor Rev. 2009; 20:153–164. [PubMed: 19261538]
22. Aleman-Muench GR, Soldevila G. When versatility matters: activins/inhibins as key regulators of immunity. Immunol Cell Biol. 2012; 90:137–148. [PubMed: 21537340]
23. Dalton S. Signaling networks in human pluripotent stem cells. Curr. Opin. Cell Biol. 2013; 25:241–246. [PubMed: 23092754]
24. Jones CP, Gregory LG, Causton B, Campbell GA, Lloyd CM. Activin A and TGF-β promote T(H)9 cell-mediated pulmonary allergic pathology. J. Allergy Clin. Immunol. 2012; 129:1000.e3–1010.e3. [PubMed: 22277204]
25. Huber S, et al. Activin a promotes the TGF-beta-induced conversion of CD4+CD25− T cells into Foxp3+ induced regulatory T cells. J Immunol. 2009; 182:4633–4640. [PubMed: 19342638]
26. Ogawa K, Funaba M, Chen Y, Tsujimoto M. Activin A functions as a Th2 cytokine in the promotion of the alternative activation of macrophages. J Immunol. 2006; 177:6787–6794. [PubMed: 17082592]
27. Robson NC, et al. Activin-A: a novel dendritic cell-derived cytokine that potently attenuates CD40 ligand-specific cytokine and chemokine production. Blood. 2008; 111:2733–2743. [PubMed: 18156495]
28. Erämaa M, Hurme M, Stenman UH, Ritvos O. Activin A/erythroid differentiation factor is induced during human monocyte activation. J Exp Med. 1992; 176:1449–1452. [PubMed: 1402687]
29. Ogawa K, Funaba M, Mathews LS, Mizutani T. Activin A stimulates type IV collagenase (matrix metalloproteinase-2) production in mouse peritoneal macrophages. J Immunol. 2000; 165:2997–3003. [PubMed: 10975808]
30. Schmitt N, et al. IL-12 receptor β1 deficiency alters in vivo T follicular helper cell response in humans. Blood. 2013; 121:3375–3385. [PubMed: 23476048]
31. Abe Y, Minegishi T, Leung PCK. Activin receptor signaling. Growth Factors. 2004; 22:105–110. [PubMed: 15253386]
32. Tsuchida K, et al. Activin signaling as an emerging target for therapeutic interventions. Cell Commun. Signal. 2009; 7:15. [PubMed: 19538713]
33. Sáez de Guinoa J, Barrio L, Mellado M, Carrasco YR. CXCL13/CXCR5 signaling enhances BCR-triggered B-cell activation by shaping cell dynamics. Blood. 2011; 118:1560–1569. [PubMed: 21659539]
34. Kroenke MA, et al. Bcl6 and Maf Cooperate To Instruct Human Follicular Helper CD4 T Cell Differentiation. J Immunol. 2012; 188:3734–3744. [PubMed: 22427637]
35. Chevalier N, et al. CXCR5 Expressing Human Central Memory CD4 T Cells and Their Relevance for Humoral Immune Responses. J Immunol. 2011; 186:5556–5568. [PubMed: 21471443]
36. Locci M, et al. Human circulating PD-1+CXCR3-CXCR5+ memory Tfh cells are highly functional and correlate with broadly neutralizing HIV antibody responses. Immunity. 2013; 39:758–769. [PubMed: 24035365]
37. Morita R, et al. Human blood CXCR5(+)CD4(+) T cells are counterparts of T follicular cells and contain specific subsets that differentially support antibody secretion. Immunity. 2011; 34:108–121. [PubMed: 21215658]
38. Moens L, Tangye SG. Cytokine-Mediated Regulation of Plasma Cell Generation: IL-21 Takes Center Stage. Front Immunol. 2014; 5:65. [PubMed: 24600453]
39. Travis MA, Sheppard D. TGF-β Activation and Function in Immunity. Annu Rev Immunol. 2013
40. Oestreich KJ, Mohn SE, Weinmann AS. Molecular mechanisms that control the expression and activity of Bcl-6 in TH1 cells to regulate flexibility with a TFH-like gene profile. Nat Immunol. 2012; 13:405–411. [PubMed: 22406686]
41. Johnston RJ, Choi YS, Diamond JA, Yang JA, Crotty S. STAT5 is a potent negative regulator of TFH cell differentiation. J Exp Med. 2012; 209:243–250. [PubMed: 22271576]

42. Ray JP, et al. The Interleukin-2-mTORc1 Kinase Axis Defines the Signaling, Differentiation, and Metabolism of T Helper 1 and Follicular B Helper T Cells. Immunity. 2015

43. Inman GJ, et al. SB-431542 is a potent and specific inhibitor of transforming growth factor-beta superfamily type I activin receptor-like kinase (ALK) receptors ALK4, ALK5, and ALK7. Mol. Pharmacol. 2002; 62:65–74. [PubMed: 12065756]

44. Herbertz S, et al. Clinical development of galunisertib (LY2157299 monohydrate), a small molecule inhibitor of transforming growth factor-beta signaling pathway. Drug Des Devel Ther. 2015; 9:4479–4499.

45. Shen MM, et al. Expression of LIF in transgenic mice results in altered thymic epithelium and apparent interconversion of thymic and lymph node morphologies. EMBO J. 1994; 13:1375–1385. [PubMed: 8137821]

46. Tran DQ, Ramsey H, Shevach EM. Induction of FOXP3 expression in naive human CD4+FOXP3 T cells by T-cell receptor stimulation is transforming growth factor-beta dependent but does not confer a regulatory phenotype. Blood. 2007; 110:2983–2990. [PubMed: 17644734]

47. Marshall HD, et al. The tumor growth factor beta signaling pathway is critical for the formation of CD4 T follicular helper cells and isotype-switched antibody responses in the lung mucosa. Elife. 2015; 4

48. León B, Bradley JE, Lund FE, Randall TD, Ballesteros-Tato A. FoxP3+ regulatory T cells promote influenza-specific Tfh responses by controlling IL-2 availability. Nat Comms. 2014; 5:3495.

49. McCarron MJ, Marie JC. TGF-β prevents T follicular helper cell accumulation and B cell autoreactivity. J. Clin. Invest. 2014; 124:4375–4386. [PubMed: 25157822]

50. Bentebibel S-E, et al. Induction of ICOS+CXCR3+CXCR5+ TH Cells Correlates with Antibody Responses to Influenza Vaccination. Sci Transl Med. 2013; 5:176ra32–176ra32.

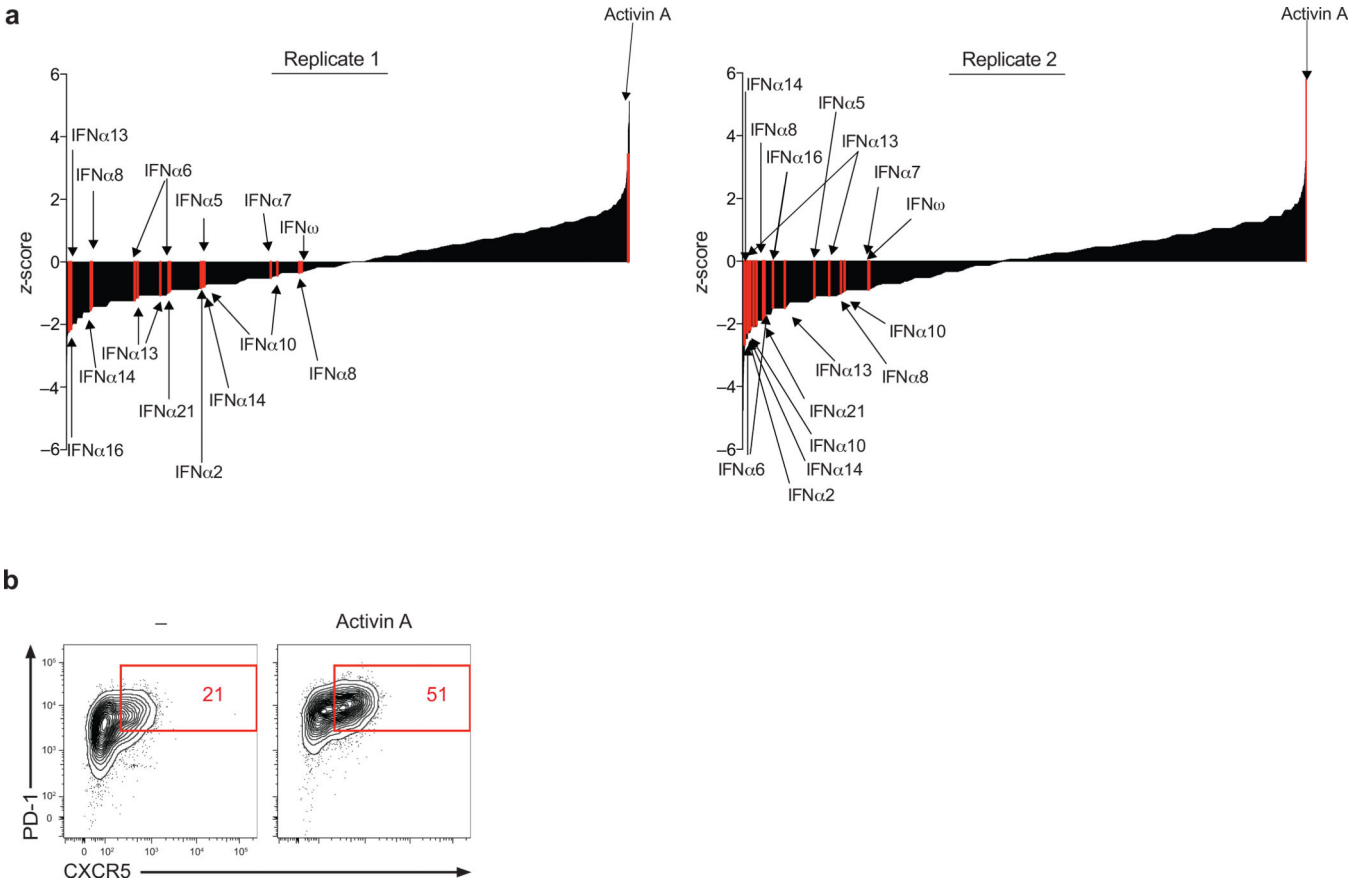

Figure 1. High throughput screening identifies activin A as a potent regulator of human T_{FH} cell differentiation

(a) Primary screen results. Enrichment of PD-$1^{+}$$CXCR5^{+}$ cell induction is reported as *z*-score for each recombinant protein from 8 × 384 well plates. Activin A and 11 type I interferon family proteins are shown in red. (b) Expression of CXCR5 and PD-1 from a screen repeat experiment re-testing activin A from secretomics library for its capacity to induce T_{FH}-like differentiation. The data are representative of 2 independent replicates.

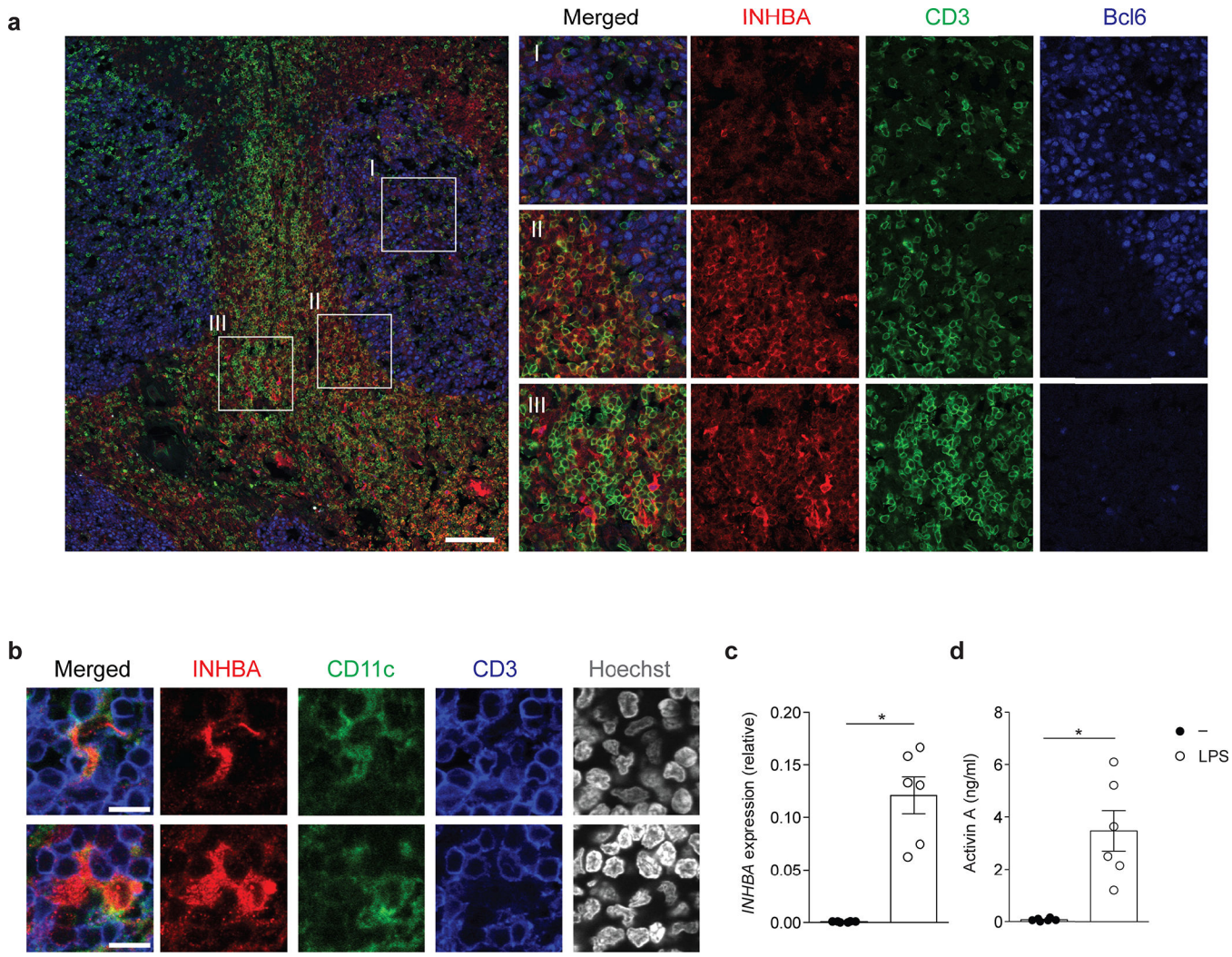

Figure 2. INHBA is present in sites relevant for T_{FH} cell differentiation and can be produced by myeloid cells

(a) Confocal microscopy of INHBA expression in human tonsils stained with anti-INHBA (red) anti-Bcl6 (blue) and anti-CD3 (green). An overlay from one donor representative of six is shown on the left panel. Enlarged images on the right show representative INHBA expression in (I) a germinal center, (II) the T cell-B cell border and (III) T cell areas. Scale bar=100μm.(b) Confocal microscopy of INHBA expression in tonsil $CD11c^+$ DCs. Tonsil sections were stained with anti-INHBA (red) anti-CD11c (green), anti-CD3 (blue) and counterstained with Hoechst. An overlay from one donor representative of two is shown on the left panel. The images were enlarged from a larger section depicted in Supplementary Fig 2b. Scale bar=10μm.(c) *INHBA* expression relative to *GAPDH* in purified monocytes cultured with and without E.Coli LPS (100ng/ml) for 4 h. The relative expression is shown as 2^-ΔCt. (d) Quantification of activin A secretion from purified monocytes cultured with and without *E. coli* LPS (100ng/ml) for 48h. Data (c,d) are combined from 2 independent experiments (n=6). Each symbol indicates an individual sample. * $P < 0.05$ (two-tailed Wilcoxon matched-pairs signed ranked test). (c,d; error bars represent mean and s.e.m.)

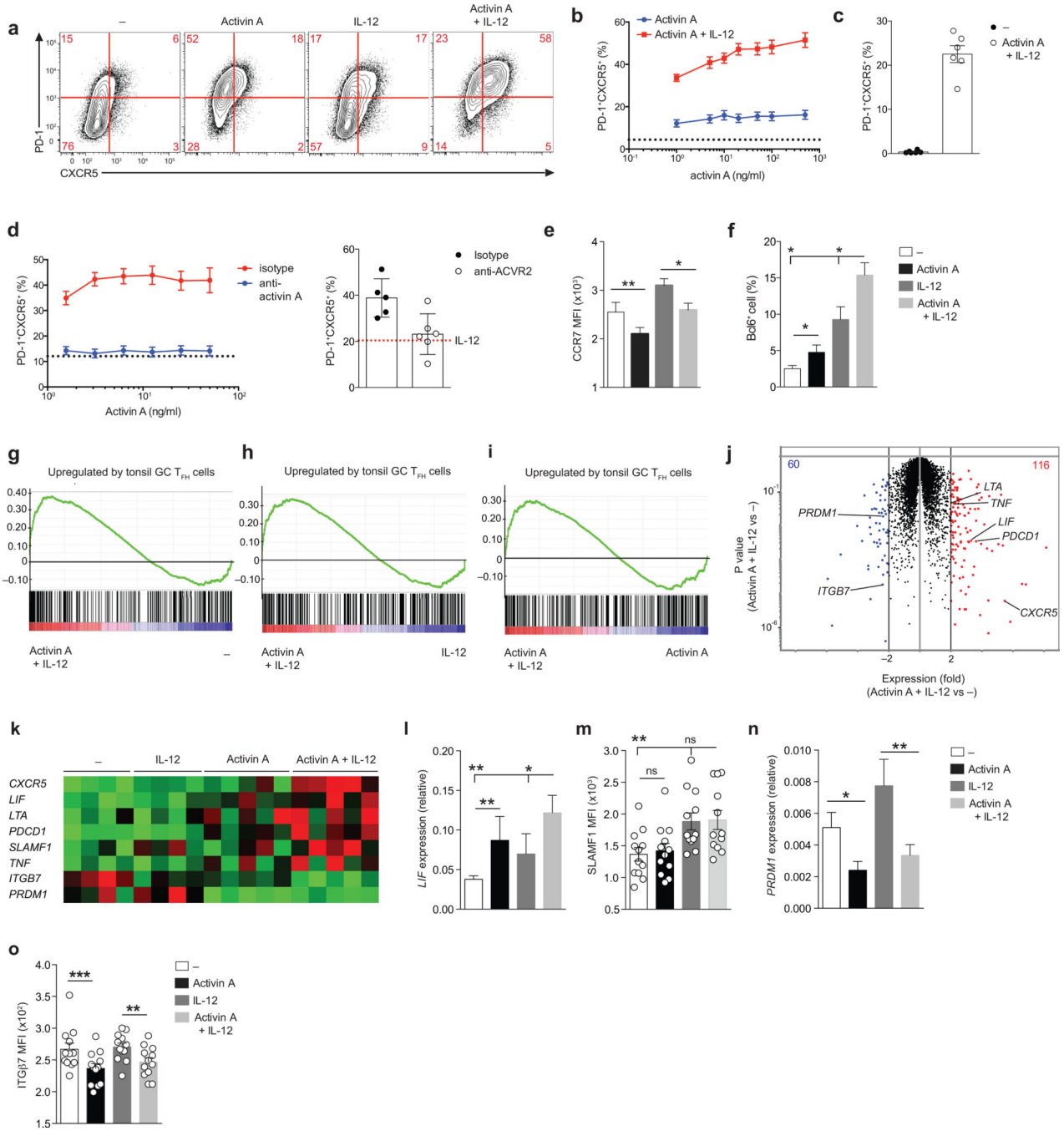

Figure 3. Activin A synergizes with IL-12 and molds the human T_{FH} gene program

(a) Flow cytometry of naïve $CD4^+$ T cells stimulated by anti-CD3/CD28 beads for 5 d, in the presence of commercial human recombinant activin A, with or without IL-12. Cells stimulated with beads only (−) were used as control. Numbers in quadrants indicate percentage of cells in the outlined areas. (b) Frequency of PD-1^+CXCR5^+ cells as in (a). The dotted line shows the average basal induction of PD-1^+CXCR5^+ cells induced by beads only (−) from 13 donors. (c) Frequency of PD-1^+CXCR5^+ cells following 10 d of *in vitro* differentiation as in (a). (d) Left: frequency of PD-1^+CXCR5^+ cells from bead-activated

naïve $CD4^+$ T cells cultured *in vitro* with different doses of activin A combined with a fixed amount of IL-12 for 5 d in the presence of anti-activin A (block) or isotype control antibody (isotype). Dotted lines indicate the average percentages of $PD\text{-}1^+CXCR5^+$ cells induced by IL-12 with isotype control antibody. Right: frequency of $PD\text{-}1^+CXCR5^+$ cells from bead-activated naïve $CD4^+$ T cells differentiated with activin A and IL-12, or IL-12 only (red dotted line, average value), in the presence of pan anti-ACVR2 or isotype control antibody. (e) Mean fluorescence intensity (MFI) of CCR7 on cells cultured as in (a). (f) Frequency of Bcl6 intranuclear expression on cells differentiated as in (a). (g-i) Enrichment of tonsil GC T_{FH} signature genes in genes upregulated by activin A + IL-12 cultured cells in comparison to beads only (−) (g), IL-12 (h) or activin A only (i) stimulated cells. (j) RNAseq gene expression of cells differentiated as in (a) for 3d. Red: activin A + IL-12 versus – fold change (FC) > 2; blue: activin A + IL-12 versus – FC < −2). (k) RNAseq gene expression of selected T_{FH} signature genes from (j). (l) *LIF* expression relative to *ACTB* in cells cultured as in (j)(m) MFI of SLAMF1 expression on cells cultured as in (j)(n) *PRDM1* expression relative to *ACTB* in cells cultured as in (j) (o) MFI of ITGβ7 expression on cells cultured as in (j).Data in (b-f) and (l-o) data are from 2 or more independent experiments (n=6 or higher). * $P < 0.05$, ** $P < 0.01$ and *** $P < 0.001$ (two-tailed Wilcoxon matched-pairs signed ranked test). In (c), (e, f) and (l-o) bars show mean and s.e.m..

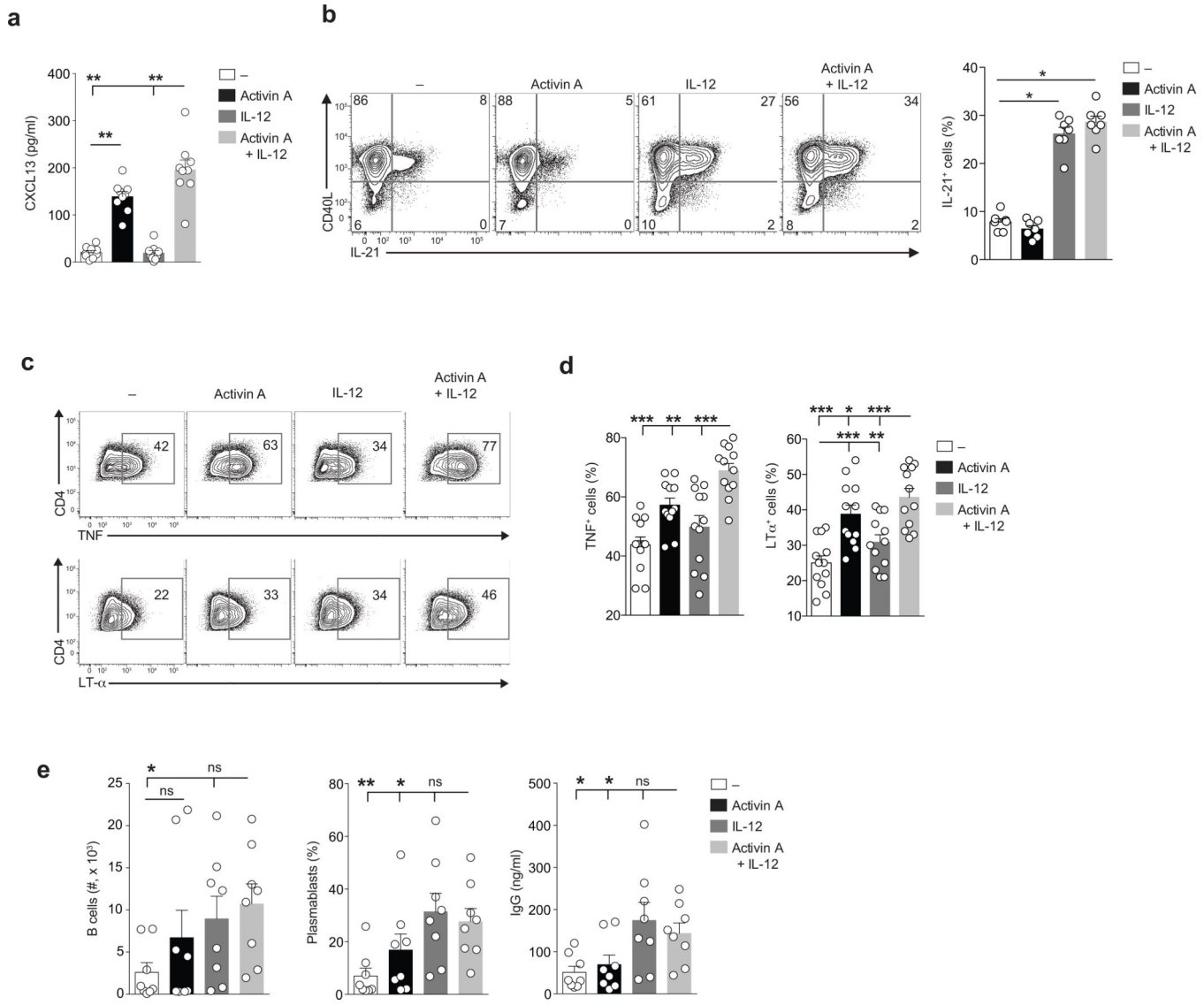

Figure 4. CD4$^+$ T cells differentiated with activin A acquire functional signature molecules of T$_{FH}$ cells

(a) Production of CXCL13 by naïve CD4$^+$ T cells stimulated by plate bound anti-CD3 and hrICOS-L chimera, in the presence of human recombinant activin A, with or without IL-12 for 5 d. (b) Flow cytometry of CD40L and IL-21 intracellular expression on naive CD4$^+$ T cells stimulated stimulated by anti-CD3/CD28 beads for 5 d, in the presence of activin A, with or without IL-12 and re-stimulated on day 5 with PMA/Ionomycin. Numbers in quadrants indicate percentage of cells in the outlined areas. (c) Flow cytometry of TNFα and LTα intracellular expression on cells differentiated as in (b) for 3 d and stimulated on day 3 with PMA/Ionomycin. Numbers in quadrants indicate percentage of cells in the outlined areas. (d) Frequency of cells in (c). (e) Absolute numbers of live CD19$^+$ B cells (left plot), frequency of plasmablasts (CD19$^+$CD20^{lo}CD38$^+$ cells, center plot), and secreted IgG generated from coculture of memory B cells with autologous naïve CD4$^+$ T cells differentiated as in (b) for 3d in the presence of SEB. In all (a-e) data are from 3 or more

independent experiments (n=7 or more), and bars are mean and s.e.m.. * $P < 0.05$, ** $P < 0.01$ and *** $P < 0.001$. (a-d: two-tailed Wilcoxon matched-pairs signed ranked test; e: one-tailed Wilcoxon matched-pairs signed ranked test).

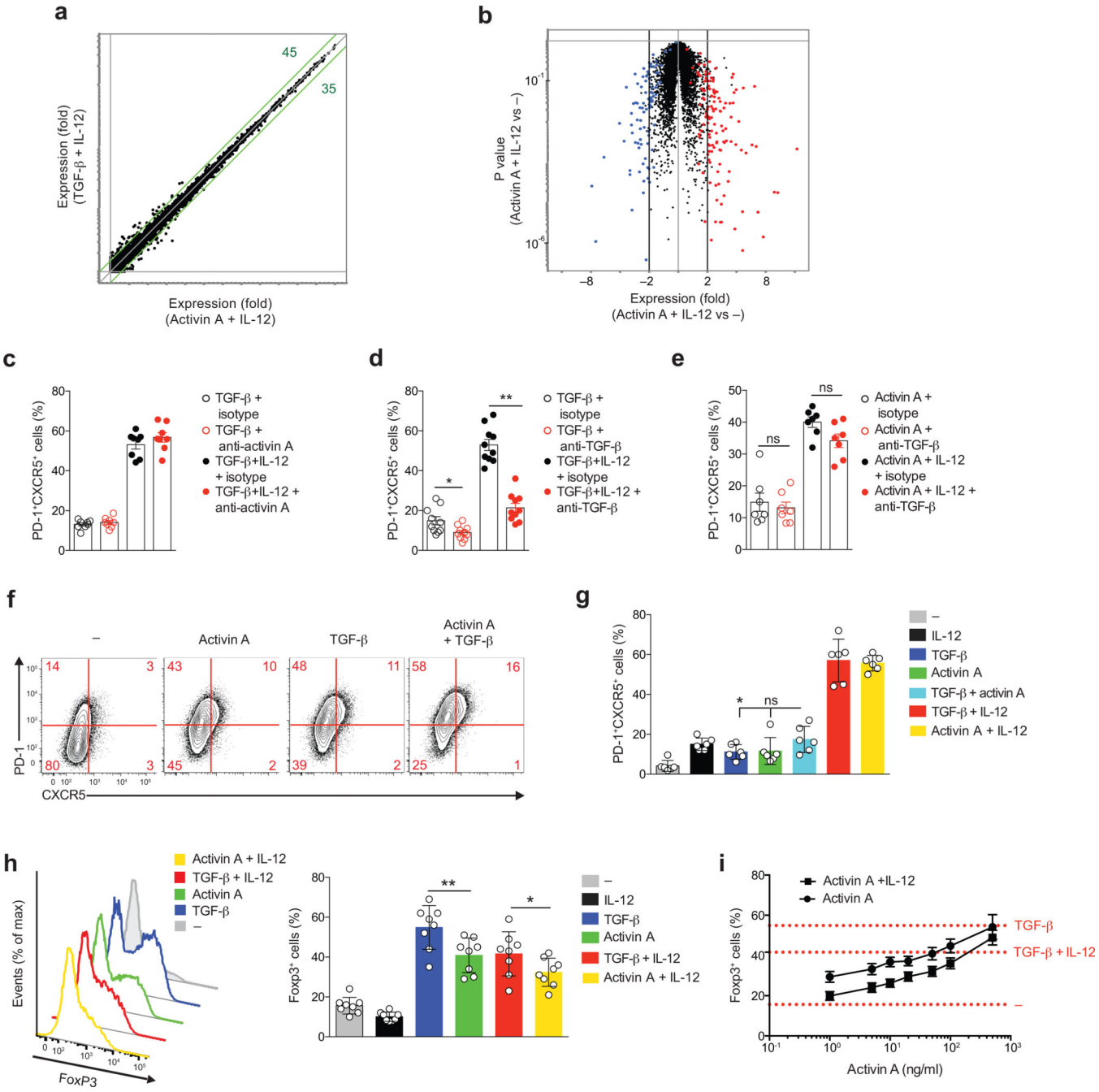

Figure 5. Activin A and TGF-β act independently from each other to drive *in vitro* T_{FH} cell differentiation

(a) RNA-seq gene expression on naive $CD4^+$ T cells stimulated by anti-CD3/CD28 beads for 3 d, in the presence of activin A + IL-12 or TGF-β + IL-12.(b) RNA-seq gene expression on cells from (a). Red: TGF-β + IL-12 versus –, fold change (FC) > 2), blue: TGF-β + IL-12 versus –, FC < −2. (c) Frequency of PD-1^+CXCR5^+ naïve $CD4^+$ T cells stimulated by anti-CD3/CD28 beads for 5 d with TGF-β, alone or with IL-12, in the presence of anti-activin A or isotype control antibody. (d-e) Frequency of PD-1^+CXCR5^+ naïve $CD4^+$ T cells stimulated by anti-CD3/CD28 beads for 5 d with TGF-β and TGF-β + IL-12 (d) or activin A

and activin A+IL-12 (e), in the presence of anti- TGFβ or isotype control antibody. (f) Flow cytometry of naïve $CD4^+$ T cells stimulated by anti-CD3/CD28 beads for 5 d, in the presence of activin A, with or without TGF-β. Cells stimulated with beads only (−) were used as control. Numbers in quadrants indicate percentage of cells in the outlined areas. (g) Quantification of (f). (h-i) Expression of FoxP3 on naïve $CD4^+$ T cells differentiated *in vitro* for 5d with different cytokine combinations. In (c-i) data are cumulative from 3 or more experiments (n=6 or more). * $P < 0.05$, ** $P < 0.01$ and *** $P < 0.001$ (Two-tailed Wilcoxon matched-pairs signed ranked test).

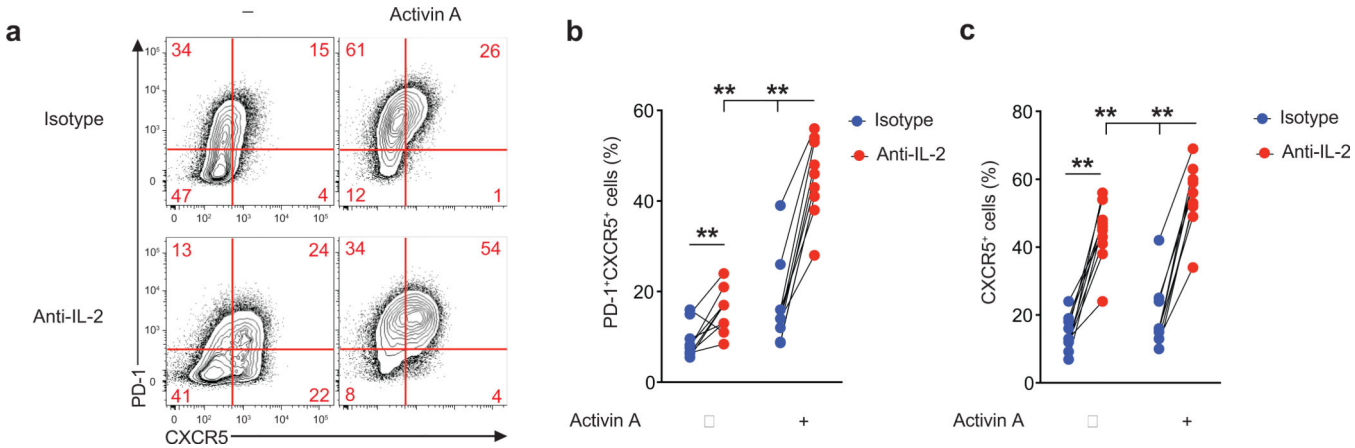

Figure 6. IL-2 antagonizes activin A driven T_{FH} cell differentiation

(a-c) Flow cytometry of naïve $CD4^+$ T cells stimulated by anti-CD3/CD28 beads for 5d with activin A, or beads only (−), in the presence of anti-IL-2, or isotype control antibody. Numbers in quadrants indicate percentage of cells in the outlined areas. Data are cumulative from 3 independent experiments (n=10). ** $p<0.01$ (Two-tailed Wilcoxon matched-pairs signed ranked test).

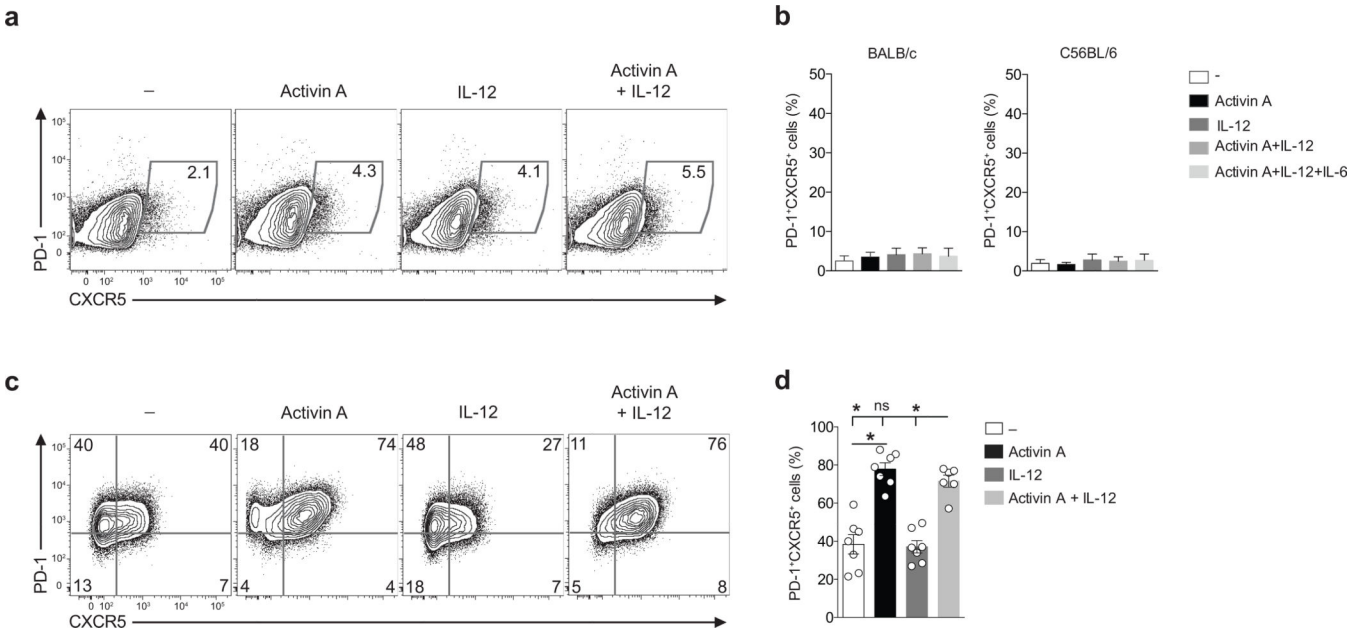

Figure 7. The role of activin A in T_{FH} cell differentiation is conserved for non-human primate, but not mouse $CD4^+$ T cells

(a) Flow cytometry of naïve $CD4^+$ T cells from BALB/c or C57BL/6 mice cultured *in vitro* for 5 d with IL-12, activin A, activin A and IL12 or medium only (−), in the presence of plate-bound anti-CD3 and anti-CD28. Numbers in gates indicate percentages of $PD\text{-}1^+$ $CXCR5^+$ cells.(b) Frequency of cells in (a). (c) Flow cytometry of naïve $CD4^+$ T cells from rhesus macaque activated by plate bound anti-CD3 and anti-CD28 in the presence of activin A, with or without IL-12, or medium only (−) for 5d. Numbers in quadrants indicate percentage of cells in the outlined areas.(d) Frequency of cells in (c). In (a-d) data are from 4 or more independent experiments (n=4 or more). Bars are mean and s.e.m. * $p<0.05$ (Two-tailed Wilcoxon matched-pairs signed ranked test).

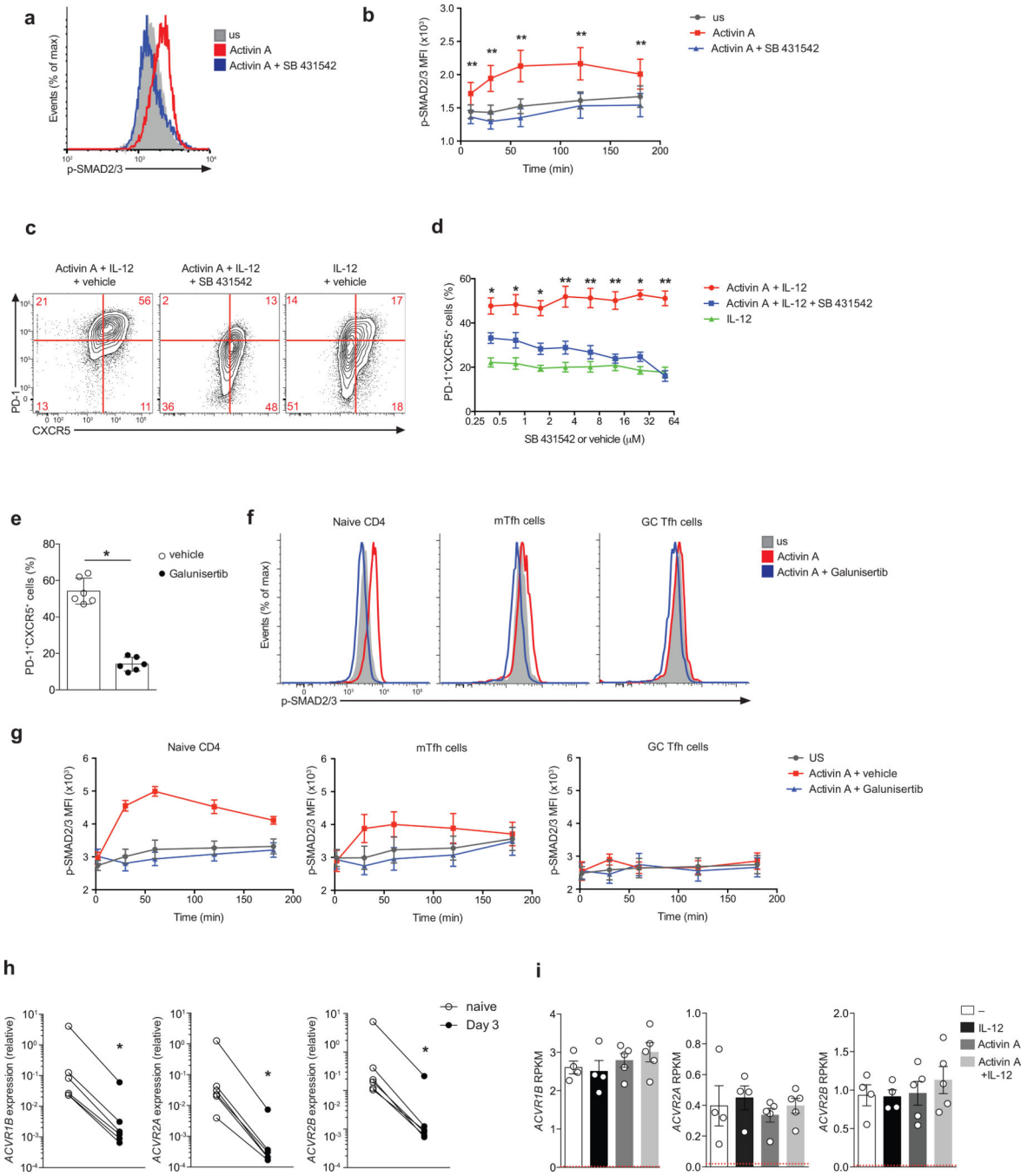

Figure 8. Activin A activity is mediated by an ALK4-SMAD2/3 pathway

(a-b) Flow cytometry of phosphorylated-SMAD2/3 (p-SMAD) by human naïve CD4$^+$ T cells following stimulation for 60 min (a) or up to 180 min (b) with activin A (red), activin A + SB 431542 (blue) and in unstimulated cells (US, grey). (c) Flow cytometry of human naïve CD4$^+$ T cells differentiated for 5 d with activin A + IL-12 or IL-12 only in the presence of SB 431542 (50μM) or vehicle (DMSO). Numbers in quadrants indicate percentage of cells in the outlined areas.(d) Frequency of PD-1$^+$CXCR5$^+$ on cells differentiated as in (c) in the presence of different doses of SB 431542 (50μM) or vehicle

(DMSO). (e) Frequency of PD-1^{+}CXCR5^{+} on cells naïve CD4^{+} T cells differentiated for 5 d with activin A + IL-12 in the presence of Galunisertib or vehicle (DMSO). (f-g) Flow cytometry of phosphorylated-SMAD2/3 (p-SMAD) by tonsillar naïve CD4^{+} T cells (CD4^{+}CD45RO^{-}), mT$_{FH}$ (CD4^{+}CD45RO^{+}PD-1^{int}CXCR5^{int}) and GC T$_{FH}$ cells (CD4^{+}CD45RO^{+}PD-1^{hi}CXCR5^{hi}) following stimulation for 60 min (f) or up to 180 min (g) with activin A (red), activin A + Galunisertib (blue) and in unstimulated cells (US, grey). (h) Type I (*ACVR1B*) and Type II (*ACVR2A* and *ACVR2B*) activin A receptor expression relative to *GAPDH* on naïve CD4^{+} T cells *ex vivo* (naïve), or upon 3 d following *in vitro* anti-CD/CD28 bead stimulation. (i) RNA-seq gene expression of *ACVR1B, ACVR2A* and *ACVR2B* on naïve CD4^{+} T cells stimulated with antiCD3/CD28 beads for 3 d with activin A, with or without IL-12, IL-12 and beads only (−). *NGFR* average expression by cells differentiated with beads only (−) is shown in red. Bars are mean and s.e.m.. In (c-h) data are cumulative from 2 or more experiments (n=6 or more). * $P < 0.05$, ** $P < 0.01$ and *** $P < 0.001$ (Two-tailed Wilcoxon matched-pairs signed ranked test).